Journal of Photochemistry & Photobiology, A: Chemistry 414 (2021) 113270

Contents lists available at ScienceDirect

Journal of Photochemistry & Photobiology, A: Chemistry

journal homepage: www.elsevier.com/locate/jphotochem

A turn-on fluorescent probe based on π-extended coumarin for imaging endogenous hydrogen peroxide in RAW 264.7 cells

Yu-Bo Wang, Hui-Zhen Luo, Cheng-Yun Wang *, Zhi-Qian Guo, Wei-Hong Zhu *

Key Laboratory for Advanced Materials and Institute of Fine Chemicals, School of Chemistry and Molecular Engineering, East China University of Science and Technology, 130 Meilong Road, Shanghai, 200237, PR China

ARTICLE INFO

Keywords:
Fluorescent probe
Coumarin
Endogenous
Hydrogen peroxide
Bioimaging

ABSTRACT

Hydrogen peroxide (H_2O_2), one of reactive oxygen species, is implicated in the biological process of oxidative metabolism and signal transduction. However, the detection of H_2O_2 in *vivo* is restricted by background interference in the context of fluorescence probes. In this work, by regulating the intramolecular charge transfer (ICT) process, a novel "turn-on" fluorescent probe **BC-OB** is constructed based on a π-extended coumarin and a p-dihydroxyborylbenzyloxycarbonyl moiety as an optimized hydrogen peroxide reactive site. The mechanism was identified by HPLC and HRMS: after the H_2O_2-mediated oxidation of aryl boronate moiety on **BC-OB**, the hydrolysis resulted in a release of the π-extended coumarin with specific fluorescence response. The sensitive response of probe **BC-OB** to H_2O_2 was revealed by high fluorescence quantum yields (Φ up to 0.68) and low detection limit (0.47 μM) due to the enhancement of the ICT process. Further, probe **BC-OB** could successfully trap endogenous H_2O_2 in RAW 264.7 cells, promising it would be used as an efficient indicator for imaging H_2O_2.

1. Introduction

Involved in many physiological and pathological micro-environmental variation, reactive oxygen species (ROS) consist of plentiful reactive oxygen-containing molecules or ions [1–4]. Hydrogen peroxide (H_2O_2) is one of the reactive oxygen species derived from nicotinamide adenine dinucleotide phosphate (NADPH) oxidase. H_2O_2 can be generated from dismutation of $O_2^{\cdot-}$, either spontaneously or via the action of superoxide dismutase (SOD) [5] and get involved in many biological process of oxidative metabolism and signal transduction [6–10]. As a signaling molecule, H_2O_2 can readily permeate biological membranes and its level in cell is closely related to cell proliferation, differentiation, migration, and apoptosis [6]. Abnormal level of H_2O_2 concentration in biological system can significantly impact ones' health and underlie several common diseases further, such as obesity, diabetes, Alzheimer's disease, cardiovascular, neurodegenerative disorders, even cancer [11–15]. Hence, for exploring the impact of H_2O_2 on related diseases, it is crucial to design new kinds of effective, specific, and simple tools to monitor H_2O_2 concentration.

In recent decades, many methods have been proposed for the visualization of intracellular H_2O_2, including electrochemical methods, spectrophotometry, chemi-luminescence and fluorescent probes [16, 17]. From the present understanding, the analytical methods for visualization of H_2O_2 is increasingly dominated by fluorescence imaging with advantages of high specificity, non-invasive examination, organelle localization, and reversible detection for clinic medicine research, and various detection strategies on H_2O_2-mediated reaction emerged, such as sulfonic ester hydrolysis, benzyl oxidation and boronate oxidation [18–28]. Since Chang et al. pioneered the use of aromatic boronic ester oxidation as a trigger to detect H_2O_2 [29,30], strategies based on boronate deprotection have been extensively adopted, offering probes for H_2O_2 detection at different locations [31–36]. Yet, in terms of biological applications, some of fluorescent probes could not meet the ideal requirements on detection of H_2O_2 due to their reaction activity, detection sensitivity, and interference of auto-fluorescence in complex biological environment. [37,38]. Thus, developing a simple fluorescent probe with good sensitivity to quantitative detection of H_2O_2, as well as weakening self-quenching, is of considerable significance.

Herein, a new colorimetric and "turn-on" fluorescent probe **BC-OB** was designed, which takes advantages of high selectivity and high fluorescence quantum yields to detect H_2O_2 at the cellular level (Scheme 1). In our strategy, an arylboronate handle as a H_2O_2 transponder was introduced due to the efficient reactivity and good biocompatibility. To regulate the intramolecular charge transfer (ICT) effect, a π-extended

* Corresponding authors.
E-mail addresses: cywang@ecust.edu.cn (C.-Y. Wang), whzhu@ecust.edu.cn (W.-H. Zhu).

https://doi.org/10.1016/j.jphotochem.2021.113270
Received 4 January 2021; Received in revised form 24 March 2021; Accepted 25 March 2021
Available online 27 March 2021

benzothiazolyl moiety was assembled with the coumarin fluorophore. Moreover, carbonate group was optimized as an electron-withdrawing linker to quench the fluorescence of coumarin signally before the response of H_2O_2. After the addition of H_2O_2, the fluorescence of probe **BC-OB** exhibited a significant 10-hold enhancement. With the auxiliary means of bio-imaging microscope, probe **BC-OB** was allowed to monitor H_2O_2 in cells.

2. Experimental section

2.1. General information

All solvents and chemical reagents were observed from commercial providers in analytical grade and could be utilized without purification. The information about synthetic compounds, instruments, spectral measurement, cells culture and cells imaging were assessed in supporting information.

2.2. Synthesis of probe *BC-OB*

The synthetic route to probe **BC-OB** is demonstrated in Scheme 2. The compounds of 3-benzothiazolyl-7-hydroxycoumarin (**BC-OH**) and 4-(4,4,5,5-tetramethyl-1,3,2-dioxaborolan-2-yl) benzyl carbonochloridate (**BP-OCl**) could be easily synthesized by condensation reaction and Suzuki reaction respectively according to previous literature [39,40]. The structure of synthetic compounds was characterized by ^{1}H NMR, ^{13}C NMR, and HRMS (See ESI, Figs. S1–S7). The probe was then obtained by substitution reaction of **BC-OH** and **BP-OCl**. After dissolving **BC-OH** (300 mg, 1.02 mmol) in super dry dichloromethane (15 mL), Et_3N (0.3 mL, 4.03 mmol) was dropped in ice bath as acid-binding agent. The diluted **BP-OCl** (602 mg, 2.03 mmol) was gently added into the reaction system to make sure the reaction proceed smoothly. Then the mixture solution was concentrated under vacuum after 8 h, further purified by column chromatography separation (DCM:PE 2:1) to observe final product as a yellow-green solid (285 mg, 78 %). ^{1}H NMR (400 MHz, $CDCl_3$) δ (ppm): 9.07 (s, 1 H), 8.12 (d, J =8.0 Hz, 1 H), 8.02 (d, J =8.0 Hz, 1 H), 7.86 (d, J =8.0 Hz, 2 H), 7.75 (d, J =8.8 Hz, 1 H), 7.56 (t, J =16.4 Hz, 1 H), 7.46 (d, J =8.0 Hz, 3 H), 7.36 (d, J =2.4 Hz, 1 H), 7.24 (d, J =2.4 Hz, 1 H), 5.33 (s, 2 H), 1.35 (s, 12 H); ^{13}C NMR (150 MHz, DMSO-$_{d6}$) δ (ppm): 159.62, 159.51, 154.40, 152.54, 152.44, 144.04, 140.71, 137.11, 136.84, 135.22, 135.08, 130.24, 127.67, 127.47, 126.58, 126.09, 125.50, 122.94, 1121.80, 119.86, 118.62, 116.89, 109.73, 84.00, 70.83, 65.32, 24.87. HRMS (ESI) m/z: $[M+H]^+$ calcd for $[C_{30}H_{26}BNO_7S+H]^+$, 556.1601; found, 556.1592.

3. Results and discussion

3.1. Design of probe *BC-OB*

In general, coumarin-derived fluorescent probes combining with other functional groups were always designed by modification at the 7-position and 3-position [41–44]. The present strategy to construct a new colorimetric and "turn-on" fluorescent probe relies on regulating ICT in virtue of an asymmetric-modified coumarin-derived platform, to optimize the spectra behavior of probe **BC-OB** in absorption and fluorescence (Scheme 1). Meanwhile, due to the efficient reactivity and good biocompatibility, boronate, as a H_2O_2 transponder, was introduced at the 7-position of coumarin, which could be easily attacked by hydrogen peroxide and transform to generate phenol under neutral and alkaline conditions. In addition, an assumption was made that introducing benzothiazolyl moiety at the 3-position of coumarin, which could enhance the ICT process by constructing a more planar structure to elevate the charge-separated resonance of excited geometries. The carbonate group was also selected to link the arylboronate handle with fluorophore rather than ether group, as the negative charge on the phenolate could more easily transfer to an electron-withdrawing carbonyl of carbonate group than an ether group, and form unprotected alcohol [41,45–47]. Notably, at the 7-position of coumarin, carbonate group possessed a stronger electron-donor effect than that of ether group, and obviously blocked ICT process [48]. Therefore, to establish a "turn-on" fluorescent response platform, p-dihydroxyborylbenzyloxycarbonyl moiety was selected as an optimized reactive site.

3.2. Spectral properties

Initially, the solvent effect to fluorophore BC-OH was investigated with common solvents including toluene, DCM, THF, MeCN, DMF, DMSO and PBS buffer (20 mM, pH, 7.4). The results were shown in Fig. S8a–b and the corresponding data were collected in Table S2. Moreover, the fluorescent intensity and response time in different contents of DMSO in PBS buffer (20 mM, pH, 7.4) was also presented in Fig. S8c–d. Took the fluorescence behavior and solubility into account, PBS with 20 % DMSO was selected to detect H_2O_2 for further measurements.

Then, probe **BC-OB** incubated with different concentrations of H_2O_2 (0–100 μM) was measured in PBS buffer (20 mM, pH, 7.4) with 20 % DMSO (Fig. 1). As can be observed in Fig. 1a, a free probe without the addition of H_2O_2 had a featured absorption peak around 365 nm and it displayed no shark absorption peak at around 475 nm. The reason may contribute to the 7-hydroxyl group of the coumarin was esterified by phenylboronic, thus blocked ICT process. Upon increasing the concentration of H_2O_2 (0–100 μM), probe **BC-OB** exhibited a significant red-shift, the absorption peak at 475 nm gradually rose up, and the absorption peak at 365 nm declined. The solution color changed from initially colorless to yellow-green (Fig. 1a). Furthermore, the fluorescence emission at 495 nm emerged with the increase of H_2O_2 concentration (0–100 μM) at the excitation of 475 nm, the phenomenon maybe caused by the oxidation-induced cleavage of p-dihydroxyborylbenzyloxycarbonyl, and its fluorescence was recoverd (Fig. 1b). Simultaneously, as shown in Fig. 1c, the fluorescence intensity at 495

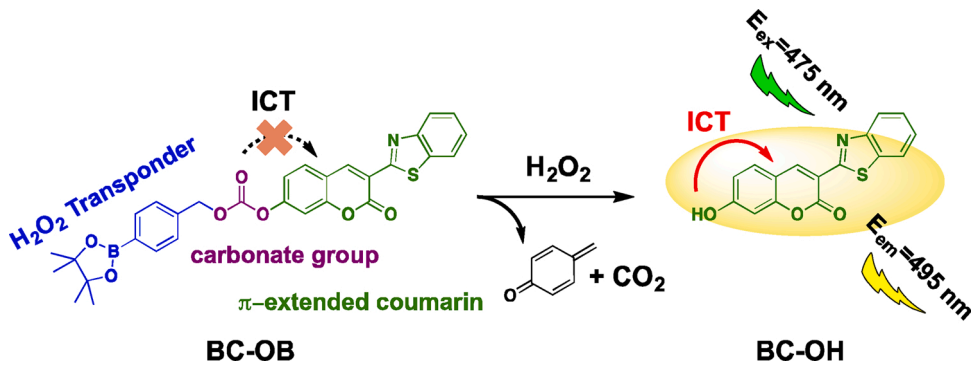

Scheme 1. Illustration of designing a "turn-on" fluorescent probe **BC-OB** based on a π-extended coumarin fluorophore for H_2O_2 detection.

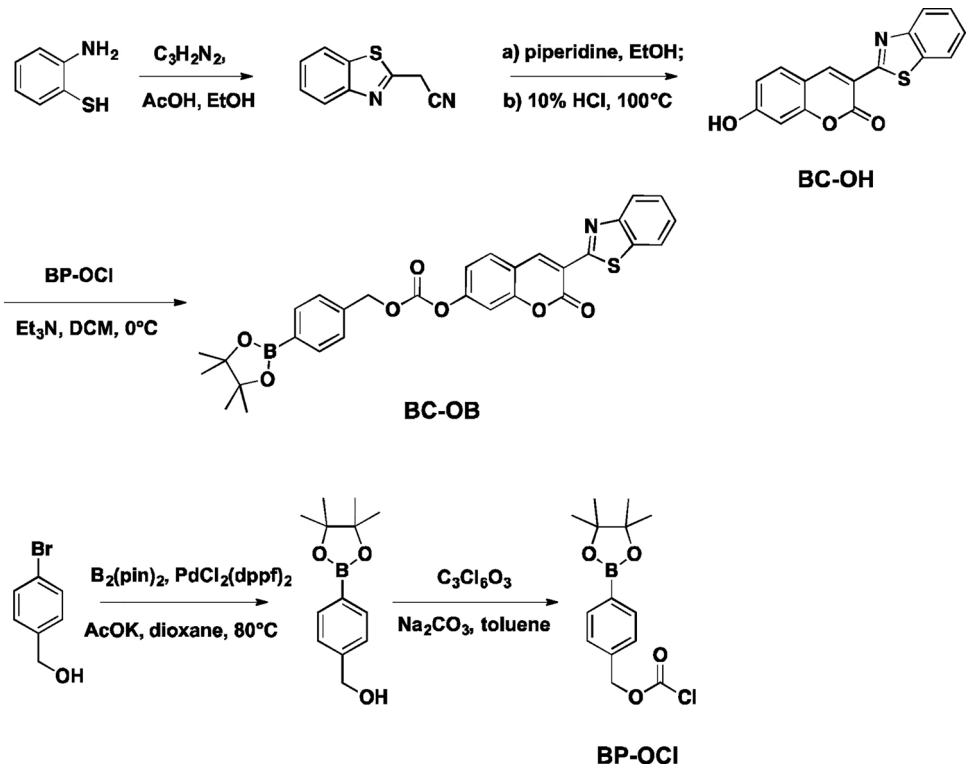

Scheme 2. The synthetic route of probe **BC-OB**.

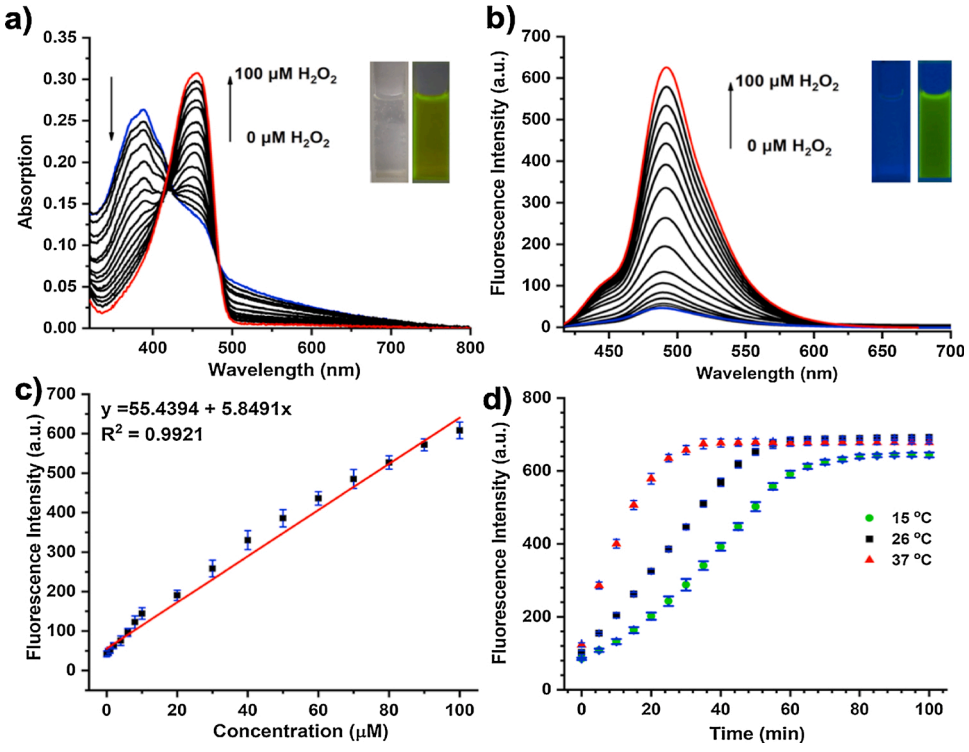

Fig. 1. a) Absorption and b) fluorescence spectra of probe **BC-OB** (10 μM) with increasing equivalence of H_2O_2 (0–100 μM); c) Plots of fluorescence intensity of probe **BC-OB** (10 μM) as a function with H_2O_2 concentration (0–100 μM); d) Time dependence of fluorescence intensity for probe BC-OB (10 μM) with the addition of 100 μM H_2O_2 at different temperature (15 °C, 26 °C, and 37 °C), All the tests were conducted in PBS buffer solution (20 mM, pH 7.4) with 20 % DMSO, λ_{ex} =475 nm, λ_{em} =495 nm.

nm was significantly correlated in a linear manner with H_2O_2 concentration from 0 μM to 100 μM ($R^2 = 0.9921$). Owing to the planarity of the probe structure preventing a nonfluorescent twisted ICT state [49,50], the fluorescence quantum yields significantly raised to 0.68 (Table S1). The evident emission response towards H_2O_2 could be explained by the distinct electron redistribution before and after reacting with H_2O_2, for p-dihydroxyborylbenzyloxycarbonyl was utilized to efficiently regulating the ICT process of coumarin fluorophore.

Subsequently, the response time of probe **BC-OB** towards H_2O_2 and the photostability of probe **BC-OB** was also investigated. In the presence of 100 μM of H_2O_2, the emission peak at 495 nm exhibited a 10-fold fluorescence enhancement, and the response time was shortened from

80 min to 30 min when temperature was changed from 15 °C to 37 °C (Fig. 1d). When excited at 475 nm for 3 h, its fluorescence intensity did not change before and after reacting with H_2O_2 (Fig. S9), thereby confirming probe **BC-OB** is photostable. According to the equation in ESI, the detection limit was measured as 0.47 μM, which was much lower in contrast to the physiological H_2O_2 concentration level in inflamed cell and organization (10–100 μM) [51]. These data indicated that probe **BC-OB** was sensitive to H_2O_2, and possessed potential application for detecting H_2O_2.

3.3. Selectivity and pH effect

To evaluate the specificity of probe **BC-OB** towards H_2O_2, it was incubated with different potential representative species, including typical reactive oxygen species (ClO^-, $^{\bullet}OH$, $ROO^{\bullet}$, $O_2^{-\bullet}$), reactive nitrogen species (NO, $ONOO^-$), reactive sulfur species (SO_3^{2-}, S^{2-}, Cys, Hcy, GSH) and common ions (Na^+ Mg^{2+} Ca^{2+}, SO_4^{2-}, NO_3^-, AcO^-). In consideration of DMSO being a scavenger of hydroxyl radicals [52], measurements were conducted in PBS buffer (20 mM, pH 7.4), and the results were collected in Fig. 2. As shown in Fig. 2a–b, only the addition of H_2O_2, the absorption of probe **BC-OB** exhibited obvious red-shift (from 365 nm to 475 nm), and its fluorescence obviously enhanced (495 nm), while other biologically relevant species exhibited slight or no variation in both the absorption and fluorescence behavior. Compared with other analytes, the probe displayed outstanding selectivity toward H_2O_2 (Fig. 2c). These data demonstrated that probe **BC-OB** possessed high selectivity towards H_2O_2.

In order to research the stability of probe **BC-OB** under physiological conditions, the pH impacts on probe **BC-OB** were also investigated, and the results were collected in Fig. 2d. As shown in Fig. 2d, the fluorescent behavior of probe **BC-OB** was stable in physiological pH and increased slightly at the pH value from 8.5 to 10.5. It demonstrated that probe BC-OB would not be affected by pH variations in physiological conditions. The fluorescent behavior of BC-OB + H_2O_2 at different pH values (3.5–10.5) exhibited a similar trend with that of BC-OH (see Fig. S10), indicating that the fluorescence variation of BC-OB + H_2O_2 at different pH was predominantly dependent on the property of the product BC-OH. As presented in Fig. 2b, the intensity of fluorescence at 495 nm showed a strong uptrend in pH value from 5.5 to 7.5 and became stable at pH value from 8.0 to 10.5. The effective response of probe **BC-OB** displayed in neutral and alkaline environments could be ascribed to the BC-O- deprotonated from product BC-OH [53]. These results suggested that probe **BC-OB** could perform with high reactivity and stability under physiological conditions, and with possible applications in the visualization of exogenous and endogenous H_2O_2 in complex living organisms.

3.4. Proposed sensing mechanism

To identify the sensing mechanism of probe **BC-OB** responding to H_2O_2, high-performance liquid chromatography (HPLC) was utilized on the samples with probe **BC-OB**, reaction mixtures of probe **BC-OB** with H_2O_2 and pure **BC-OH**. As depicted in Fig. 3, **BC-OB** and **BC-OH** exhibited a single peak with retention times of 4.90 and 2.52 min, respectively. After adding H_2O_2 into **BC-OB** solution for 30 min, the peak of **BC-OB** fell, while a new peak belonging to **BC-OH** rose, which proofed that the product of **BC-OB** reacting with H_2O_2 is **BC-OH**. In addition, the mass spectral analysis in Fig. S11 also verified the same proposed mechanism as HPLC chromatograms. A mass peak at 294.0224 was found in the mixture of **BC-OB** and H_2O_2, which was almost the same as the exact mass fragment of **BC-OH** (*m/z* for $[M-H]^-$: 294.0225). As presented in Scheme 3, the generation of **BC-OH** could be divided into two steps according to the prior research [32,48]: i) H_2O_2 attacked arylboronate moiety of **BC-OB** and broke the B—C bond; and ii) the rearrangement of self-immolative linker was activated, upon which a fast hydrolysis occurred on the carbonate group to release the free **BC-OH**, thereby effectuating fluorescence recovery for the coumarin.

3.5. Fluorescence imaging of exogenous and endogenous H_2O_2 in living cells

For the assessment of the cellular toxicity of probe **BC-OB** as an imaging tools in living cells, probe **BC-OB** was firstly employed to

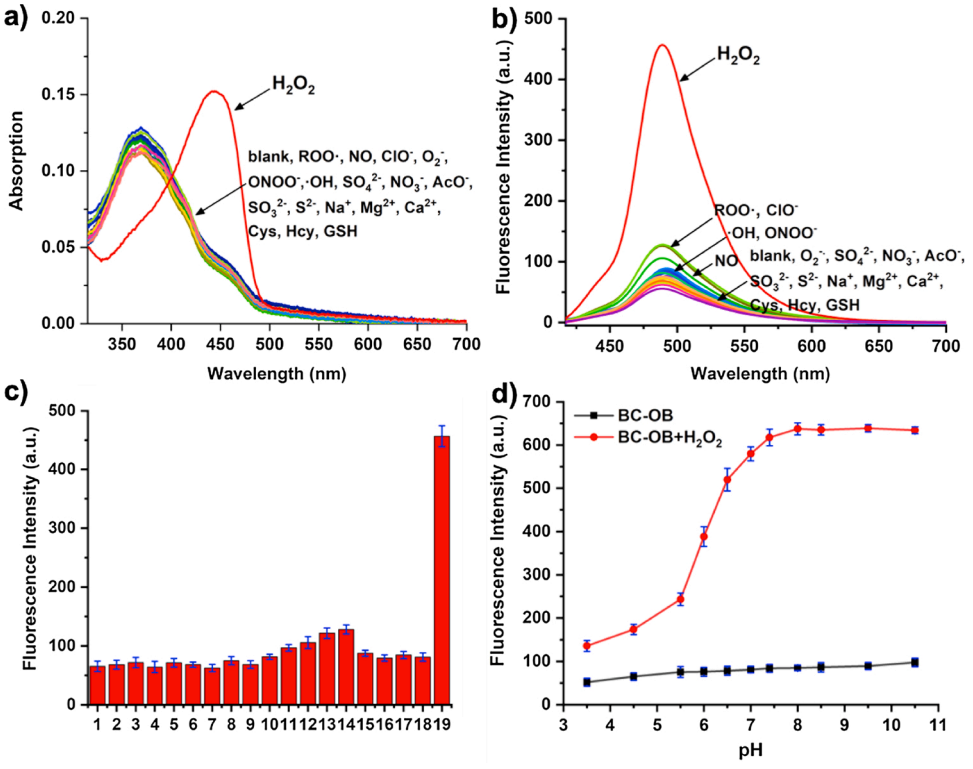

Fig. 2. a) Absorption and b) Fluorescent spectra of probe **BC-OB** (10 μM) in PBS buffer (20 mM, pH, 7.4) to potential representative species; c) Probe **BC-OB** (10 μM) fluorescence response to potential representative species: 1. blank, 2. Na^+(500 μM), 3. Mg^{2+} (500 μM), 4. Ca^{2+} (500 μM), 5. SO_4^{2-} (500 μM), 6. NO_3- (500 μM), 7. AcO- (500 μM), 8. SO_3^{2-} (500 μM), 9. S^{2-} (500 μM), 10. $^{\bullet}OH$ (100 μM), 11. ONOO- (100 μM), 12. NO (100 μM), 13. ROO·(100 μM), 14. ClO- (100 μM), 15. O_2-$^{\bullet}$ (100 μM), 16. Cys (500 μM), 17. Hcy (500 μM), 18. GSH (500 μM), 19. H_2O_2 (10 μM) in PBS buffer (20 mM, pH 7.4) during a 75 min incubation at room temperature. d) Fluorescence intensity of probe **BC-OB** (10 μM) at different pH values (3.5–10.5) in absence (black) and presence (red) of H_2O_2 (100 μM) in a PBS buffer solution with 20 % DMSO (λ_{ex} =475 nm, λ_{em} =495 nm).

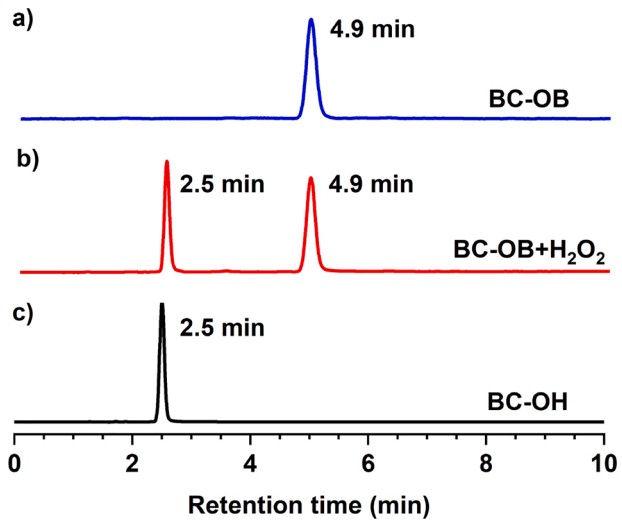

Fig. 3. HPLC chromatogram. **a)** represented the sample of probe **BC-OB**; b) represented the sample of probe **BC-OB** (10 μM) reacting with H_2O_2 (50 μM) after 30 min and c) represented the sample of **BC-OH**. Condition of HPLC: eluent: H_2O/MeOH (5:95, v/v); detection wavelength: a) 475 nm, b-c) 365 nm; injection volume: 50 μL.

incubate with murine RAW 264.7 macrophages by MTS [3-(4,5-dimethyl-2-yl)-5-(3-carboxymethoxyphenyl)-2-(4- sulfophenyl)-2H-tetrazolium] cell proliferation assay. The probe was incubated at different concentrations ranging from 2.5 μM to 20 μM (Fig. S12), and the results suggested that probe **BC-OB** possesses prominent biocompatibility. Inspired by the low cytotoxicity of probe **BC-OB**, probe **BC-OB** was then applied for fluorescence imaging of exogenous H_2O_2 in the model of RAW 264.7 cells. After incubating cells with probe **BC-OB** (10 μM) for half an hour, there was a slight fluorescence in the cells without the addition of stimulants, which could be ascribed to the existence of endogenous H_2O_2 in RAW 264.7 cells (Fig. 4a). Further treating probe-loaded cells with exogenous H_2O_2 for another 30 min, exogenous stimulants led to effectuating a noble bright-green fluorescence enhancement at 475 nm excitation (Fig. 4b), which verified the mechanism of H_2O_2-mediated boronate cleavage and the release of **BC-OH** fluorescence. Simultaneously, fluorescence imaging of probe **BC-OB** (10 μM) with different H_2O_2 concentration (0 μM, 50 μM, 100 μM) in RAW 264.7 macrophages was also studied (Fig. S13), the results indicated that the higher the concentration of exogenous H_2O_2, the stronger the fluorescence intensity.

Based on the good fluorescent performance and biocompatibility in living cells, the feasibility of probe **BC-OB** responding to endogenous H_2O_2 was further explored. As shown in Fig. 4c, phorbol 12-myristate 13-acetate (PMA, 1 μg mL^{-1}) was added to RAW 264.7 cells to induce more intracellular ROS, and its fluorescence signal significantly enhanced. Moreover, TEMPO (2,2,6,6-tetramethylpiperidine-1-oxyl, 100 μM) was adopted for pretreatment with RAW 264.7 cells to scavenge intracellular ROS, and then incubate with **BC-OB**. Compared with the fluorescence signal from RAW 264.7 cells incubated with probe **BC-OB** only, the fluorescence signal from RAW 264.7 cells incubated with scavenger TEMPO and probe **BC-OB** was obviously declined (Fig. 4d), which demonstrated the existence of endogenous H_2O_2 in RAW 264.7 cells. These images clearly illustrated that probe **BC-OB** is an invaluable tool for imaging endogenous H_2O_2 in RAW 264.7 cells.

4. Conclusions

In summary, a colorimetric and "turn-on" fluorescent probe **BC-OB** was designed, which equipped a π-extended coumarin as fluorophore and a p-dihydroxyborylbenzyloxycarbonyl moiety as an optimized hydrogen peroxide reactive site. Probe **BC-OB** exhibited distinct absorption and fluorescence performance with low detection limit (0.47 μM) and high fluorescence quantum yields (Φ = 0.68) both in the solution and in the living cells, benefiting from the ICT process. The fluorescent behavior of probe **BC-OB** was stable in physiological pH and exhibited good response in neutral and alkaline environments due to the deprotonation. The sensing mechanism of 2-steps generation of **BC-OH** was clearly identified by HPLC and high-resolution mass spectroscopy. Further, the imaging results demonstrated that probe **BC-OB** could be employed in the detection of endogenous H_2O_2 in RAW 264.7 cells. Hence, fluorescent probe **BC-OB** possessed the potential application as an efficient indicator for imaging H_2O_2.

Author statement

Yu-Bo Wang: Conceptualization, Methodology, Experiment, Investigation, Visualization, Writing-Original draft preparation.
Hui-Zhen Luo: Experiment; Investigation, Data curation.
Cheng-Yun Wang: Supervision, Writing- Reviewing and Editing.
Zhi-Qian Guo: Visualization, Validation.
Wei-Hong Zhu: Supervision, Writing- Reviewing and Editing.

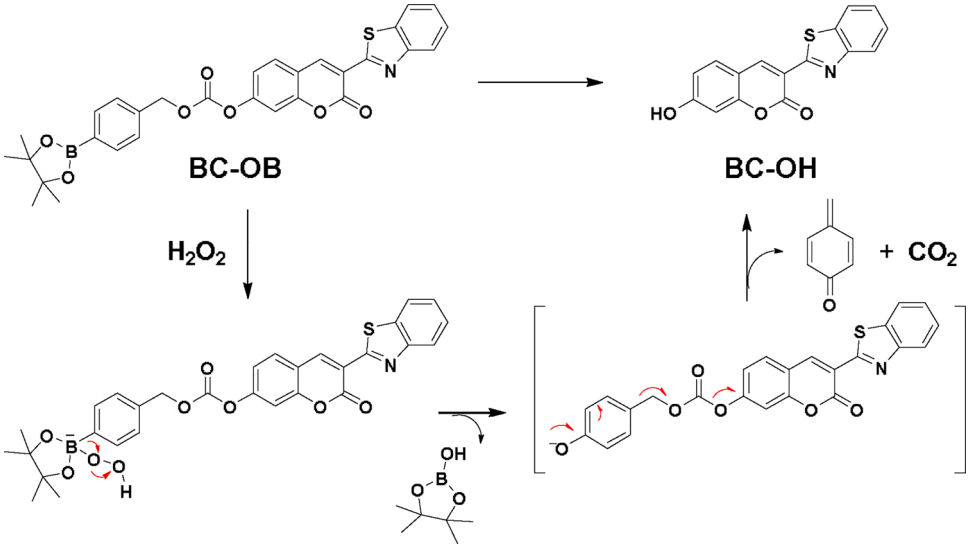

Scheme 3. Proposed sensing mechanism of probe **BC-OB** with H_2O_2.

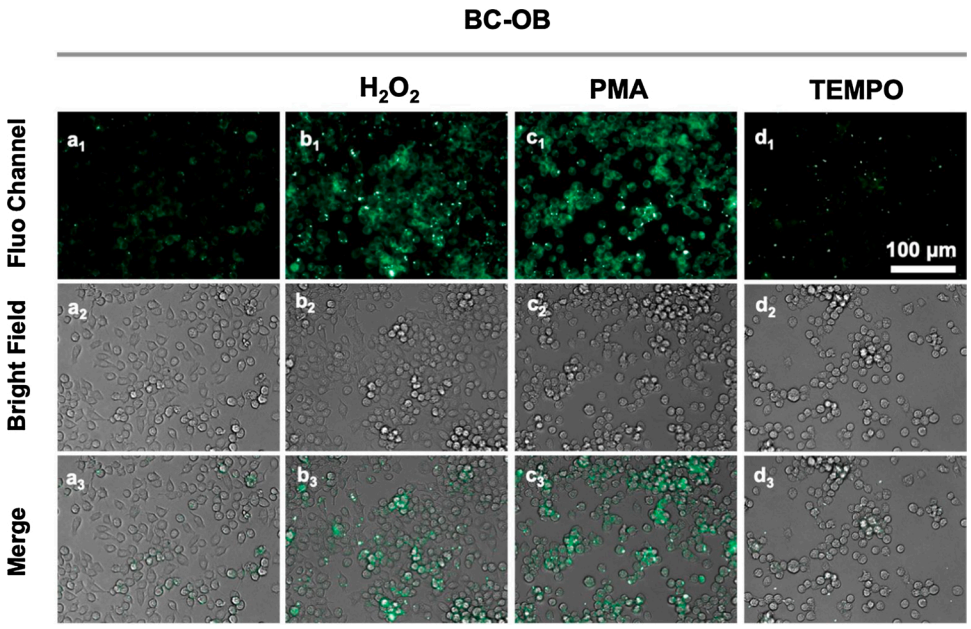

Fig. 4. Fluorescence imaging of RAW 264.7 macrophages. (**a_1-a_3**) represented RAW 264.7 incubated with probe **BC-OB** only (10 μM) for 30 min; (**b_1-b_3**) represented RAW 264.7 incubated with probe **BC-OB** (10 μM) for 30 min and H_2O_2 (100 μM) for another 30 min; (**c_1-c_3**) represented RAW 264.7 incubated with probe **BC-OB** (10 μM) for 30 min and PMA (1 μg mL^{-1}) for 30 min; and (**d_1-d_3**) represented RAW 264.7 incubated with TEMPO (100 μM) for 30 min and probe **BC-OB** for 30 min, scale bar: 100 μM.

Declaration of Competing Interest

The authors declare that they have no known competing financial interests or personal relationships that could have appeared to influence the work reported in this paper.

Acknowledgments

The authors are grateful to financial support from Natural Science Foundation of Shanghai (No. 16ZR1408000) and the National Key Program ofChina (No. 2016YFA0200302). And the authors would like to thank Professor Xiao-Peng He for living cells experiment.

Appendix A. Supplementary data

Supplementary material related to this article can be found, in the online version, at doi:https://doi.org/10.1016/j.jphotochem.2021.113270.

References

[1] X. Chen, X. Tian, I. Shin, J. Yoon, Fluorescent and luminescent probes for detection of reactive oxygen and nitrogen species, Chem. Soc. Rev. 40 (2011) 4783–4804.
[2] B.C. Dickinson, C.J. Chang, Chemistry and biology of reactive oxygen species in signaling or stress responses, Nat. Chem. Biol. 7 (2011) 504–511.
[3] X. Chen, F. Wang, J.Y. Hyun, T. Wei, J. Qiang, X. Ren, I. Shin, J. Yoon, Recent progress in the development of fluorescent, luminescent and colorimetric probes for detection of reactive oxygen and nitrogen species, Chem. Soc. Rev. 45 (2016) 2976–3016.
[4] A. García-Sánchez, A.G. Miranda-Díaz, E.G. Cardona-Muoz, The role of oxidative stress in physiopathology and pharmacological treatment with pro- and antioxidant properties in chronic diseases, Oxid. Med. Cell. Longev. 3 (2020) 1–16.
[5] K. Bedard, K.H. Krause, The NOX family of ROS-generating NADPH oxidases: physiology and pathophysiology, Physiol. Rev. 87 (2007) 245–313.
[6] S.G. Rhee, H_2O_2, a necessary evil for cell signaling, Science 312 (2006) 1882–1883.
[7] C.E. Paulsen, K.S. Carroll, Orchestrating redox signaling networks through regulatory cysteine switches, ACS Chem. Biol. 5 (2010) 47–62.
[8] D. Wu, A.C. Sedgwick, T. Gunnlaugsson, E.U. Akkaya, J. Yoon, T.D. James, Fluorescent chemosensors: the past, present and future, Chem. Soc. Rev. 46 (2017) 7105–7123.
[9] H. Sies, Hydrogen peroxide as a central redox signaling molecule in physiological oxidative stress: oxidative eustress, Redox Biol. 11 (2017) 613–619.
[10] Y. Htet, Z. Lu, S.A. Trauger, A.G. Tennyson, Hydrogen peroxide as a hydride donor and reductant under biologically relevant conditions, Chem. Sci. 10 (2019) 2025–2033.
[11] Y. Pak, S. Park, D. Wu, B. Cheon, H. Kim, J. Bouffard, J. Yoon, N-heterocyclic carbene boranes as reactive oxygen species-responsive materials: application to the two-photon imaging of hypochlorous acid in living cells and tissues, Angew. Chemie Int. Ed. 57 (2018) 1567–1571.
[12] R. Kohen, A. Nyska, Oxidation of biological systems: oxidative stress phenomena, antioxidants, redox reactions, and methods for their quantification, Toxicol. Pathol. 30 (2002) 620–650.
[13] T. Finkel, M. Serrano, M.A. Blasco, The common biology of cancer and ageing, Nature 448 (2007) 767–774.
[14] S.J. Dixon, B.R. Stockwell, The role of iron and reactive oxygen species in cell death, Nat. Chem. Biol. 10 (2014) 9–17.
[15] Z. Guo, Y. Ma, Y. Liu, C. Yan, P. Shi, H. Tian, W. Zhu, Photocaged prodrug under NIR light-triggering with dual-channel fluorescence: in *vivo* real-time tracking for precise drug delivery, Sci. China Chem. 61 (2018) 1293–1300.
[16] G.J. Maghzal, K.H. Krause, R. Stocker, V. Jaquet, Detection of reactive oxygen species derived from the family of NOX NADPH oxidases, Free Radic. Biol. Med. 53 (2012) 1903–1918.
[17] S. Dupre-Crochet, M. Erard, O. Nubetae, ROS production in phagocytes: why, when, and where? J. Leukoc. Biol. 94 (2013) 657–670.
[18] L. Yuan, W. Lin, Y. Xie, B. Chen, S. Zhu, Single fluorescent probe responds to H_2O_2, NO, and H_2O_2/NO with three different sets of fluorescence signals, J. Am. Chem. Soc. 134 (2012) 1305–1315.
[19] D. Kim, G. Kim, S. Nam, J. Yin, J. Yoon, Visualization of endogenous and exogenous hydrogen peroxide using a lysosome-targetable fluorescent probe, Sci. Rep. UK 5 (2015) 1–6.
[20] R. Wang, Z. Bian, D. Zhan, Z. Wu, Q. Yao, G. Zhang, Boronic acid-based sensors for small-molecule reactive species: a review, Dyes Pigments 185 (2021), 108885.
[21] N. Li, J. Huang, Q. Wang, Y. Gu, P. Wang, A reaction based one- and two-photon fluorescent probe for selective imaging H_2O_2 in living cells and tissues, Sens. Actuators B-Chem. 254 (2018) 411–416.
[22] J. Gong, D. Feng, W. Liu, J. Fang, S. Feng, A self-immolative near-infrared probe based on hemi-benzothiazolecyanine for visualizing hydrogen peroxide in living cells and mice, Dyes Pigments 185 (2020), 108954.
[23] Q. Guan, L. Shi, C. Li, X. Gao, K. Wang, X. Liang, P. Li, X. Zhu, A fluorescent cocktail strategy for differentiating tumor, inflammation and normal cells by detecting mRNA and H_2O_2, ACS Biomater. Sci. Eng. 5 (2019) 1023–1033.
[24] H. Xiao, P. Li, X. Hu, X. Shi, B. Tang, Simultaneous fluorescence imaging of hydrogen peroxide in mitochondria and endoplasmic reticulum during apoptosis, Chem. Sci. 7 (2016) 6153–6159.
[25] C. Yan, L. Shi, Z. Guo, W. Zhu, Molecularly near-infrared fluorescent theranostics for in *vivo* tracking tumor-specific chemo-therapy, Chin. Chem. Lett. 30 (2019) 1849–1855.
[26] L. Yang, Y. Zhang, X. Ren, B. Wang, Z. Yang, X. Song, W. Wang, Fluorescent detection of dynamic H_2O_2/H_2S redox event in living cells and organisms, Anal. Chem. 92 (2020) 4387–4394.
[27] W. Zhang, F. Huo, Y. Zhang, J. Chao, C. Yin, Mitochondria-targeted NIR fluorescent probe for reversible imaging H_2O_2/SO_2 redox dynamics in vivo, Sens. Actuators B-Chem. 297 (2019) 126747–126754.
[28] M.L. Odyniec, A.C. Sedgwick, A.H. Swan, M. Weber, T.M.S. Tang, J.E. Gardiner, M. Zhang, Y. Jiang, G. Kociok-Kohn, R.B.P. Elmes, S.D. Bull, X. He, T.D. James, 'AND'-based fluorescence scaffold for the detection of ROS/RNS and a second analyte, Chem. Commun. 26 (54) (2018) 8466–8469.
[29] E.W. Miller, A.E. Albers, A. Pralle, E.Y. Isacoff, C.J. Chang, Boronate-based fluorescent probes for imaging cellular hydrogen peroxide, J. Am. Chem. Soc. 127 (2005) 16652–16659.

[30] C.D. Bryan, C. Huynh, C.J. Chang, A palette of fluorescent probes with varying emission colors for imaging hydrogen peroxide signaling in living cells, J. Am. Chem. Soc. 132 (2010) 5906–5915.
[31] Y. Urano, M. Kamiya, K. Kanda, T. Ueno, K. Hirose, T. Nagano, Evolution of fluorescein as a platform for finely tunable fluorescence probes, J. Am. Chem. Soc. 127 (2005) 4888–4894.
[32] D. Zheng, Y. Yang, H. Zhu, Recent progress in the development of small-molecule fluorescent probes for the detection of hydrogen peroxide, TrAc-Trend Anal. Chem. 118 (2019) 625–651.
[33] B.N.G. Giepmans, S.R. Adams, M.H. Ellisman, R.Y. Tsien, The fluorescent toolbox for assessing protein location and function, Science 312 (2006) 217–224.
[34] H. Zhu, J. Fan, J. Du, X. Peng, Fluorescent probes for sensing and imaging within specific cellular organelles, Acc. Chem. Res. 49 (2016) 2115–2126.
[35] R. Wang, C. Yan, H. Zhang, Z. Guo, W. Zhu, In *vivo* real-time tracking of tumor-specific biocatalysis in cascade nanotheranostics enables synergistic cancer treatment, Chem. Sci. 11 (12) (2020) 3371–3377.
[36] Y. Ohsaki, P. O'Connor, T. Mori, R.P. Ryan, B.C. Dickinson, C.J. Chang, Y. Lu, S. Ito, A.W. Cowley Jr., Increase of sodium delivery stimulates the mitochondrial respiratory chain H_2O_2 production in rat renal medullary thick ascending limb, Am. J. Physiol. Renal Physiol. 302 (2012) 95–102.
[37] X. Peng, F. Song, E. Lu, Y. Wang, W. Zhou, J. Fan, Y. Gao, Heptamethine cyanine dyes with a large stokes shift and strong fluorescence: a paradigm for excited-state intramolecular charge transfer, J. Am. Chem. Soc. 127 (2005) 4170–4171.
[38] Y. Yan, L. Liu, C. Li, Z. Yang, T. Yi, J. Hua, A NIR fluorescent probe based on phenazine with a large stokes shift for the detection and imaging of endogenous H_2O_2 in RAW 264.7 cells, Analyst 145 (2020) 4196–4203.
[39] K. Wang, G. Lai, Z. Li, M. Liu, Y. Shen, C. Wang, A novel colorimetric and fluorescent probe for the highly selective and sensitive detection of palladium based on Pd(0) mediated reaction, Tetrahedron 71 (2015) 7874–7878.
[40] H. Ji, L. Wu, J. Cai, G. Li, N. Gan, Z. Wang, Room-temperature borylation and one-pot two-step borylation/Suzuki-Miyaura cross-coupling reaction of aryl chlorides, RSC Adv. 8 (2018) 13643–13648.
[41] K.M. Mahoney, P.P. Goswami, A. Syed, P. Kolker, B. Shannan, E.A. Smith, A. H. Winte, Self-immolative phthalate esters sensitive to hydrogen peroxide and light, J. Org. Chem. 79 (2014) 11740–11743.
[42] X. Liang, X. Xu, D. Qiao, Z. Yin, L. Shang, Dual mechanism of an intramolecular charge transfer (ICT)-FRET-based fluorescent probe for the selective detection of hydrogen peroxide, Chem. - Asian J. 12 (2017) 3187–3194.
[43] D. Cao, Z. Liu, P. Verwilst, S. Koo, P. Jangjili, J. Kim, W. Lin, Coumarin-based small-molecule fluorescent chemosensors, Chem. Rev. 119 (2019) 10403–10519.
[44] N. Zhu, X. Guo, S. Pang, Y. Chang, X. Liu, Z. Shi, S. Feng, Mitochondria-immobilized unimolecular fluorescent probe for multiplexing imaging of living cancer cells, Anal. Chem. 92 (2020) 11103–11110.
[45] C. Li, S. Wang, Y. Huang, Q. Wen, L. Wang, Y. Kan, Photoluminescence properties of a novel cyclometalated iridium(III) complex with coumarin-boronate and its recognition of hydrogen peroxide, Dalton Trans. 43 (2014) 5595–5602.
[46] S.D. Bhagat, U. Singh, R.K. Mishra, A. Srivastava, An endogenous reactive oxygen species (ROS) - activated histone deacetylase inhibitor prodrug for cancer chemotherapy, ChemMedChem 13 (2018) 2073–2079.
[47] S. Ye, N. Hananya, O. Green, H. Chen, A. Zhao, J. Shen, D. Shabat, D. Yang, A highly selective and sensitive chemiluminescent probe for real-time monitoring of hydrogen peroxide in cells and animals, Angew. Chemie Int. Ed. 59 (2020) 14326–14330.
[48] W. Mao, M. Zhu, C. Yan, Y. Ma, Z. Guo, W. Zhu, Rational design of ratiometric near-infrared Aza-BODIPY-based fluorescent probe for in vivo imaging of endogenous hydrogen peroxide, ACS Appl. Bio Mater. 3 (2019) 45–52.
[49] K. Wang, C. Zhao, S. Guo, Y. Lu, Y. Shen, C. Wang, A coumarin-based near-infrared fluorescent probe with a large stokes shift for the sequential recognition of Ni^{2+} and CN^-: performance research and quantum calculation, J. Photochem. Photobiol. A 382 (2019), 111943.
[50] H. Li, Y. Yang, X. Qi, X. Zhou, W.X. Ren, M. Deng, J. Wu, M. Lu, S. Liang, A. T. Teichmann, Design and applications of a novel fluorescent probe for detecting glutathione in biological samples, Anal. Chim. Acta 1117 (2020) 18–24.
[51] M. Ren, D. Deng, K. Zhou, X. Kong, J. Wang, W. Lin, Single fluorescent probe for dual-imaging viscosity and H_2O_2 in mitochondria with different fluorescence signals in living cells, Anal. Chem. 89 (2017) 552–555.
[52] C. Tsai, A. Stern, J. Chiou, C. Chern, T. Liu, Rapid and specific detection of hydroxyl radical using an ultraweak chemiluminescence analyzer and a low-level chemiluminescence emitter: application to hydroxyl radical-scavenging ability of aqueous extracts of food constituents, J. Agric. Food Chem. 49 (2001) 2137–2141.
[53] B. Li, J.-B. Chen, Y. Xiong, X. Yang, C. Zhao, J. Sun, Development of turn-on fluorescent probes for the detection of H_2O_2 vapor with high selectivity and sensitivity, Sens. Actuators B-Chem. 268 (2018) 475–484.